Journal of Physics: Conference Series **2885** (2024) 012036 doi:10.1088/1742-6596/2885/1/012036

Numerical and experimental investigation of compartment fires

Rabah Mehaddi[1], **Bouaza Lafdal**[2], **Pascal Boulet**[1]
[1]Université de Lorraine, CNRS, LEMTA, F-54000, Nancy, France
[2]CERIB Fire Testing Centre, Epernon, France

E-mail: rabah.mehaddi@univ-lorraine.fr

Abstract. The present study focuses on under-ventilated compartment fires, by analysing the results of an experimental and numerical study about fires issuing from heptane pools in a compartment with an open door. The key parameters in this case are the ventilation factor (based on the door height and its area) and the pool fire diameter. To analyse the combustion regimes, the fire Heat Release Rate (HRR) is split into two parts, namely, the heat released inside and outside the compartment. To quantify these quantities, two experimental methods have been combined. The first one is based on temperature measurements inside the compartment. The second one combines measurements for the heat fluxes outside the compartment and images taken with visible cameras that provide the flame shape outside the compartment and lead to the corresponding total released flux. The experimental data have been compared to dedicated numerical simulations carried out with the CFD code Fire Dynamics Simulator. These comparisons have revealed that in a well-ventilated or moderately under-ventilated regime, integral quantities such as mean temperature, fire heat release rate inside and outside the room appear to be well predicted by the simulations. However, under the same conditions, the temperature profiles show differences that can be locally significant. This observation might be explained by a difficulty in correctly reproducing the flame dynamics and the air flow entering through the door. Furthermore, in the severely under-ventilated case, the temporal evolution of the average quantities (HRR and mean temperatures) are very poorly estimated by the simulations, as well as the local distributions. In this case the simulations predict that the combustion of all the combustible vapours occurs at the door, which does not correspond to the physical observations. Therefore, modifications of the CFD code are required to improve the simulations, probably also involving dedicated efforts on the ignition and extinction sub-models.

1. Introduction

The interaction of a fire with a structure has long been an important and much-studied problem [1, 2]. A particular but fundamental case is that of a fire in a compartment with a vertical opening (open doorway) [3]. Indeed, this problem dates back to the 50s and is still investigated today, apparently involving a simple implementation, but combining complex physical phenomena. When considering the case of a fire in a compartment, several different situations can be identified, depending on the type of fuel and the type of ventilation, which can be either of mechanical or natural type.

The situation of a closed or tight compartment where ventilation is mechanically controlled is a case where the system is forced by ventilation [4, 5, 6]. In this case, a distinction can be made between a fire issuing from the burning of a solid or liquid and a fire that issues from a gas. A

solid or liquid fuel burns as a result of its interaction with its environment, i.e. the amount of oxygen available and the effect of ambient radiation on the pyrolysis mechanism. When the fuel is injected with a gas burner, the system is forced by both ventilation and the fuel flow rate. This subject has been the focus of a numerous studies such as those by Mense et al. [7] and Beji et al [8]. This situation is more likely to be encountered in nearly-zero energy building, or in industrial buildings such as nuclear power plants.

The situation of interest in the present paper is rather the naturally ventilated compartment fire [9]. Here again, the fire may result from different types of fuels including solid/liquid and gaseous fire sources. When using a gas burner [10] the system is 'forced' by the fuel flow rate. In the case of a liquid or a solid fuel, the system is completely 'free'. This is the case in the present study in which heptane pool fires are used. This situation was considered in the pioneering research by Kawagoe [11] and Thomas [12]. One of the most important result is the distinction between different regimes depending on the ventilation allowed by the door size. For the well ventilated fires, the amount of oxygen is always sufficient to allow the combustion of all the combustible. Therefore, the fire Heat Release Rate (HRR) is controlled by the burning surfaces of the combustible in the compartment. If the air flow-rate is not sufficient to burn all the combustible inside the compartment, the fire becomes under-ventilated. In that case, the fire is controlled by the ventilation and therefore the HRR is piloted by the amount of oxygen entering into the compartment from the openings or in other words by the geometry of the openings. To account for the openings effects, Kawagoe [11] introduced the so called ventilation factor $A\sqrt{H}$ where A is the area of the opening and H is its height. In fact, Kawagoe [11] showed that the Mass Loss Rate (MLR) of the fuel inside the compartment is proportional to the ventilation factor, i.e. $MLR \propto A\sqrt{H}$. A complementary parameter is the opening factor $(A\sqrt{H})/A_T$, that accounts for the internal surface of the compartment A_T, which was introduced by Thomas and Heselden [12] [see also 3] in order to evaluate the burning rate of the fire. In addition, a demarcation between the fuel controlled fire and the ventilation controlled fire has been proposed by Thomas [13] which includes, the fuel load, the ventilation factor and the duration time of the fire. An important result is that in the ventilation controlled regime, the amount of air that could enter inside the compartment is limited by the ventilation factor. Indeed, using the theorem of Bernoulli and the mass balance, the mass flow rate of air entering into the compartment can be expressed as $\dot{m}_{in}/(A\sqrt{H}) = f(T_g/T_0)$ [see for instance 9] where T_g is the temperature of the smoke inside the compartment and T_0 is the ambient temperature. The maximum mass flow rate is expressed as

$$\dot{m}_{in}^{max} = 0.5A\sqrt{H} \tag{1}$$

Based on this last relation, the maximum HRR of the fire can be estimated using the relation

$$\dot{Q}^{max} = 0.5X_{O_2}\Delta H_{O_2}A\sqrt{H} \approx 1500A\sqrt{H} \tag{2}$$

where $X_{O_2} = 0.23$ is the oxygen mass fraction in the ambient air and $\Delta H_{O_2} = 13100kJ/kg$ is the average heat of combustion per unit of mass of oxygen [14]. As a consequence, for a growing fire, once it reaches its maximum HRR, the flames start to appear outside the compartment and could therefore cause the fire to spread to upper floors and may damage the structure outside the compartment. Note that $1500A\sqrt{H}$ is a theoretical value. It corresponds to a maximum that could be reached if all the oxygen entering the compartment meets the fuel and burns, which is highly hypothetical.

Nowadays, many engineering and research studies are based on numerical simulations. Indeed, these tools offer the advantages of a low cost and the possibility of investigating many different scenarios or configurations [15]. The so-called CFD softwares use different sub-models that have been calibrated for well ventilated conditions, but still need to be evaluated for under-ventilated conditions such as combustion sub models which were generally evaluated in normal

conditions.Among these sub-models, the extinction and ignition models are expected to play an important role in the under-ventilated conditions. Indeed, if fuel vapours are present in an oxygen-poor environment, extinction might occur. In addition, the smoke becomes rich in fuel and may reignite outside the compartment. This relatively complex physics calls for separate treatment of extinguishing and igniting processes [16, 17]. Another important feature in fire modelling is the combustion process itself, which for instance in Fire Dynamics Simulator (FDS code, used here) [18] is by default the infinitely fast chemistry controlled by the mixing process, estimated with the Eddy Dissipation Concept model.

In the present study, our aim is to analyse the ability of the FDS software to capture the effects of under-ventilation in the case of a compartment fire. Fire safety practitioners and engineers generally use the default settings of FDS. To perform this evaluation, experimental data from a test campaign carried out at the LEMTA laboratory will be used. As mentioned above, most of the physical models used in the computational software have been validated under conditions of sufficient oxygen supply. Therefore, correct predictions are expected in well-ventilated conditions. In the under-ventilated regime, the discrepancies between numerical and experimental results might increase. At what ventilation condition does the simulation code stop giving satisfactory results? Is it possible to predict this *a priori*? To help answer these questions, a series of comparisons will be carried out with measurements for temperature, oxygen concentration and HRR distributions inside and outside the compartment. The objective is to quantify how energy is distributed between the zones "inside the compartment" and "outside the compartment" when the fire is under-ventilated. A subsequent objective is to evaluate the capacity of FDS in its default version to reproduce the combustion process and the correct energy distribution.

The article is organized as follows: In §2, the experimental setup is described. In §3 The numerical model is discussed. In §4 the numerical simulations are compared with experimental data. In §5 we draw our conclusions.

2. Experimental setup

The experimental setup is shown in Figure 1. It corresponds to a parallelepipedic compartment with dimensions $47 \times 47 \times 84\, cm^3$ as shown in Figure (1-a). This compartment contains a door with a constant width of 19 cm and variable height H = [10 - 77] cm, allowing the ventilation factor to be varied. Heptane pool fires located at the center of the compartment were used as a fire source. Six circular pool diameters were used, namely: 5, 8, 9, 11, 13 and 15 cm. The mass of the heptane pools was measured using a mass balance with an accuracy of $0.01\, g$. This balance was placed underneath the compartment, supporting only the heptane pool, which was placed on a tripod. To measure the temperature inside the compartment four thermocouple trees have been placed on each corner of the compartment. Each tree contains 12 thermocouples with $0.5 mm$ bead size and spaced uniformly by a distance equal to 6 cm. The concentration of O_2 was measured using a sensor located near the pool fire as shown in Figure (1-b). A thermocouple tree has been placed at the door, with two successive thermocouples separated by a distance equal to 2 cm. Outside the compartment, three radiative sensors (Captec heat flux gauge) have been placed on the front, left and right side of the door in order to measure the radiative heat flux emitted by external flames. Two visible cameras register the flame shape.

3. Numerical simulations

Numerical simulations were carried out using FDS version 6.7.0 [18] in order to reproduce the experimental setup described in the previous section. Figure 2 gives an overview of the simulation domain. Table 1 summarizes the compartment dimensions, wall characteristics and ventilation factors considered for the simulations. The same sensors as those used during the experimental study were adopted in the numerical simulations. The simulations were carried

Figure 1. Schematic view of the experimental setup that was simulated numerically: (a) the dimensions of the compartment are shown, (b) the walls of the compartment are made transparent in the figures in order to show the sensors inside the compartment as well as the pool fire and (c) a top view is provided.

out in a prescriptive mode, i.e. the mass loss rate obtained experimentally is used as input parameter in the numerical simulation.

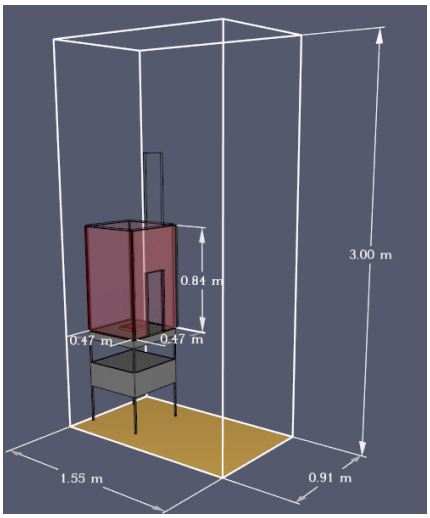

Figure 2. Illustration of the numerical domain.

Combustion is assumed to be infinitely rapid, based on the "mixed is burnt" model. This assumes that the reaction between fuel and oxygen is instantaneous, and that these two elements cannot coexist in the cell [18]. Consequently, the heat release rate will be limited by the less present species (fuel or oxygen). The reaction rate w_f can be determined as follows

$$\bar{w_f} = \rho \frac{min(Y_f, Y_{O_2}/r)}{\tau_{mix}} \tag{3}$$

Table 1. Overview of the simulation parameters.

Dimensions (m)	Material characteristics				Ventilation factor $A\sqrt{H}(m^{5/2})$	Pan size (m)
	δ (m)	ρ (kg/m^3)	C_p ($J/kg/K$)	k ($W/m/K$)		
	Internal panel (Fermacell)				0.1284, 0.11, 0.088	
$0.47 \times 0.47 \times 0.84$	0.012	1150	1200	0.32	0.0672, 0.048, 0.0312	0.11, 0.13, 0.15
	External panel (polycarbonate)				0.017, 0.006	
	0.01	1200	1440	0.2		

where Y_f and Y_{O_2} are the mass fraction of fuel and oxygen respectively, r is the stochiometric factor of the reaction, and τ_{mix} is the characteristic time scale of the mixture, taking into account the characteristic times for chemistry, diffusion, turbulence and the gravitational acceleration. Flame extinction is another important sub-model in fire modelling. FDS provides two extinction models. The model used in this study is related to the oxygen concentration. Based on an energy balance the limiting oxygen concentration can be expressed as follows:

$$Y_{O_2}^{lim} = \frac{C_p \left(T_{CFL} - T\right)}{\Delta H_c / r} \tag{4}$$

where T_{CFL} and T are the critical flame temperature (approx. 1700 K) and the temperature of the surrounding environment, respectively. C_p is the specific heat (approx. 1.1 kJ/kg/K), ΔH_c is the heat of combustion of the fuel, the ratio $(\Delta H_c/r)$ is constant (approx. 13100 (kJ/kg) according to [14]). Based on this limit, if the temperature and oxygen concentration conditions verify eq (4), the combustion reaction will take place, whereas if the oxygen concentration is below this limit, extinction occurs. Mesh resolution plays an important role in simulation quality. The criterion based on the dimensionless diameter ($\delta x < 0.1 \times D^*$) gives a good estimate of the optimal mesh size [19, 20] where D^* is defined as follows

$$D^* = \left(\frac{HRR}{C_p \rho_0 T_0 \sqrt{g}}\right)^{2/5}. \tag{5}$$

The heat release rate that was used to calculate the optimized mesh size is that of the smallest fire (4 kW). It results in an optimum mesh size of 0.01 m, which was adopted. Figure 3 shows an example of the comparison between numerical and experimental values for the temperature and oxygen concentration. This comparison confirms that the $0.1 \times D^*$ criterion provides a good estimate of the mesh size required for an optimal modeling.

4. Results and analysis

In what follows, the numerical simulations will be systematically compared to experimental data. The analysis will be based on mean quantities such as HRR, mean temperature and also on local quantities such as temperature distribution.

4.1. Combustion regimes

As explained in the introduction, two combustion regimes can be observed in a compartment fire. The first regime is called the "well-ventilated" or "fuel-controlled" regime. Combustion and heat release rate are limited by the amount of available fuel. The second regime is called the "under-ventilated" or "ventilation-controlled" regime. The flow rate of air entering in the compartment is insufficient for a complete combustion, so the heat release rate is limited by the

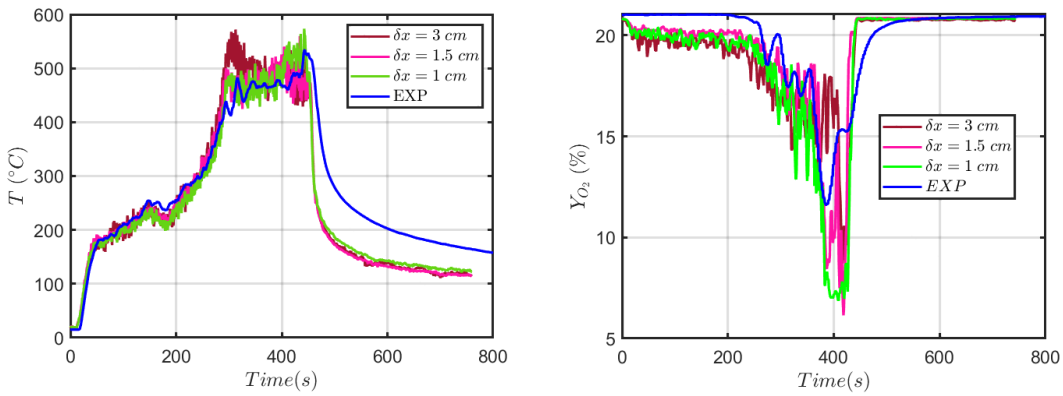

Figure 3. Temperature (below the ceiling) (a) and oxygen (b) evolution for various mesh sizes versus experimental evolution. These data are observed during a small-scale simulation/experiment with a 15 cm-diameter pan and a ventilation factor of 0.048 $m^{5/2}$.

air supply. In some cases, this second regime can lead to extinction. In the experimental tests carried out during this study, these two combustion regimes were observed. Figure 4 shows a classification of the tests according to the observed combustion regime: the green dots represent the "fuel-controlled regime", the orange dots represent the "ventilation-controlled regime" and the red dots represent the experiments for which extinction was observed. The distinction between the "fuel-controlled" regime and the "ventilation-controlled" regime is here based on the observation of external flames, which reveal the start of under-ventilated conditions. Note that, this distinction could also be made based on measurements of CO concentration which is the mark of an incomplete combustion. As expected, for the smallest pan sizes, i.e. 5, 8, 9 cm, only the "fuel-controlled regime" is observed. For diameter 11, the "fuel-controlled regime" is first observed when the opening size is high, the "ventilation-controlled" regime occurs for a lower opening size and finally the extinction occurs for the smallest opening size. For pan sizes 13 and 15 cm, we only observe the "ventilation-controlled" regime and extinction occurs for the smallest opening.

4.2. Heat release rate measurements

McCaffrey, Quintiere, and Harkleroad [21] derived a relationship coupling the average hot-layer temperature and the heat release rate inside the compartment as follows:

$$\Delta T = C \left(\frac{\dot{Q}_{in}^2}{A\sqrt{H} h_k A_T} \right)^{1/3} \tag{6}$$

where $\dot{Q}_{in}$ is the heat released inside the compartment which contributes to heat-up the smoke layer, h_k is an effective heat transfer coefficient between the smoke and the walls that is estimated as a function of a characteristic time for heat transfer $t_p = \delta^2 \rho C_p / (4k)$ as follows

$$\begin{aligned} h_k &= \sqrt{\frac{k\rho C_p}{t}} \quad \text{if} \quad t < t_p \\ h_k &= \frac{k}{\delta} \quad \text{if} \quad t > t_p \end{aligned} \tag{7}$$

where C_p is the heat capacity of the wall materials, ρ its density, k its conductivity. The constant that appears in equation 6 has been estimated to be $C = 6.85$ by McCaffrey, Quintiere,

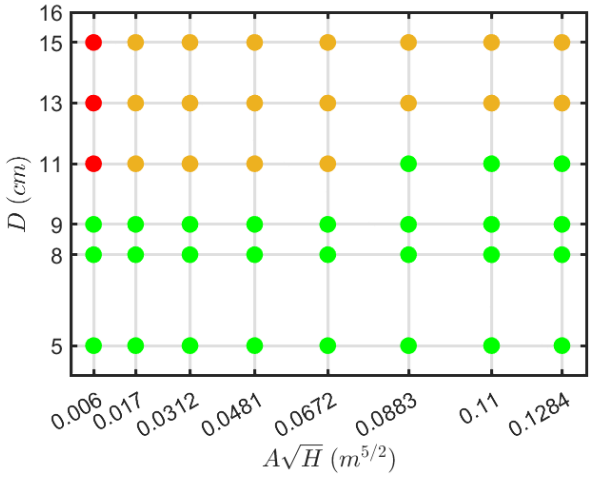

Figure 4. Classification of experiments based on combustion regime: green dots stand for "fuel-controlled" regime, orange dots for the "ventilation-controlled" regime and red dots for extinction.

and Harkleroad [21]. Note that this constant may also vary due to the fire position [22]. In the present investigation, a slightly lower value of $C = 5.80$ was obtained, based on our test campaign [23]. Since experimentally it is fairly simple to measure the temperature variation in the enclosure, this relationship can be employed in a reverse way to estimate the heat release rate inside the compartment, as follows :

$$\dot{Q}_{in} = \sqrt{\left(\frac{\Delta T}{5.8}\right)^3 \times \left(h_k A_T A\sqrt{H}\right)}\,. \tag{8}$$

Here ΔT corresponds to the smoke layer temperature difference. To determine this quantity, the method of [24, 25] is used to determine the smoke layer thickness. To calculate ΔT, all thermocouples within the hot layer are averaged. Figure (5) shows two comparisons for the heat

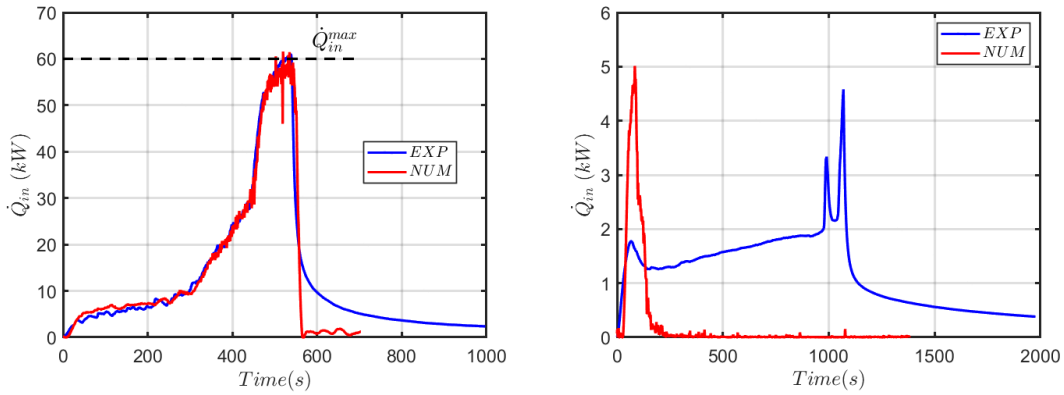

Figure 5. Comparison between the numerical and experimental variation of the heat release rate inside the compartment in the case of a 13 cm pool with a ventilation factor of (a) 0.0672 $m^{5/2}$, (b) 0.006 $m^{5/2}$.

release rate inside the compartment, with the experimental values based on equation 8 and the numerical heat release rate inside the enclosure estimated as the integral of the heat release rate over the volume of the compartment. As it can be noticed, there is a good agreement between the two estimations in Figure (5-a) for a ventilation factor equal to 0.0672 $m^{5/2}$, while a strong discrepancy appears in Figure (5-b) for a lower ventilation factor. Figure 6 presents the variation of the numerical and experimental values for the maximum heat release rate inside the compartment (corresponding to the level indicated by the dashed black line in Figure 5-a), for pool diameters equal to 11, 13, 15 cm and as a function of the ventilation factor. A reasonable agreement between numerical and experimental values can be observed. It can be concluded that FDS is able to reproduce the maximum HRR inside the compartment relatively well. But the problem lies on the time evolution of the HRR for the lowest ventilation factor (0.006 $m^{5/2}$) as shown by Figure (5-b). Indeed, the maximum HRR is similar but it does not occur at the same time. In the simulation, the HRR reaches rapidly its maximum value and after that, the flame moves to the outside of the compartment and then $\dot{Q}_{in}$ falls down to zero. In the experiment, the dynamics is slower.

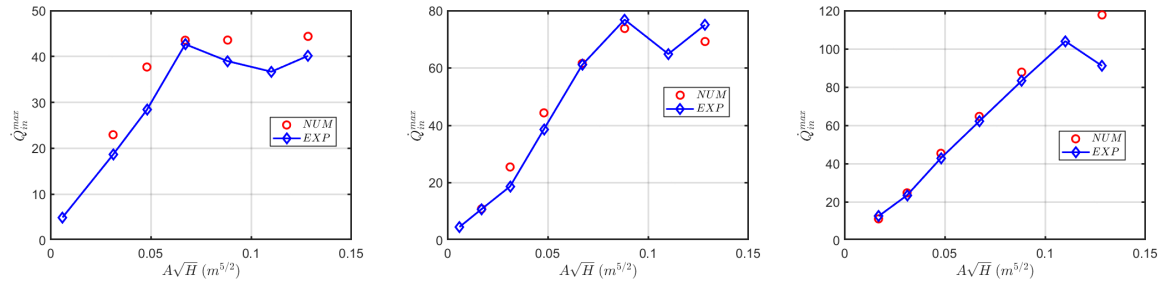

(a) D = 11 cm (b) D = 13 cm (c) D = 15 cm

Figure 6. Comparison between the numerical and experimental variation of the maximum heat release rate inside the compartment for different ventilation factors and pool diameters, (a) D= 11 cm, (b) D= 13 cm, (c) D= 15 cm.

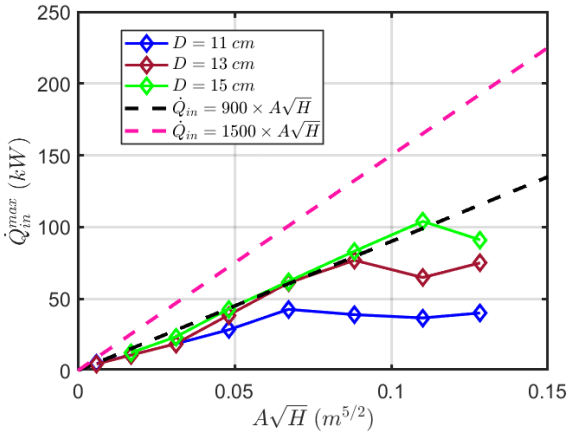

Figure 7. Variation of the maximum heat release rate inside the compartment based on experiments

Note that the maximum HRR was estimated experimentally to be $\dot{Q}_{in} = 900A\sqrt{H}$ rather than the theoretical value of $\dot{Q}_{in} = 1500A\sqrt{H}$ as can be seen in Figure 7, where the maximum

HRR inside the compartment is plotted as a function of the ventilation factor. Note that, to obtain the theoretical value of 1500, it has been assumed that all the oxygen that goes inside the compartment participates to the combustion reaction. In reality, this process depends on several parameters such as the mixing inside the compartment that is controlled by the opening geometry, the type of fire, the lower limit of oxygen that allows the combustion to occur. All these parameters contribute to reduce this value to an effective one which is found here approximately equal to 900.

Hence, it appears that the heat released by the fire outside the compartment will certainly be greater than the usual estimation obtained with the relation $\dot{Q}_{ext} = \dot{Q} - 1500 \times A\sqrt{H}$, $\dot{Q}$ standing for the total HRR inside and outside the compartment. To obtain a reliable evaluation of the external heat release rate, an experimental method based on the measurement of the radiative flux emitted by these external flames has been adopted. These measurements are then combined with an image processing method for the flame reconstruction and a Monte-Carlo method in order to provide the total radiative flux emitted by the flame, used together with the radiative fraction to provide an estimate of the total external HRR. The method is described in details in [23] and illustrated in appendix A.

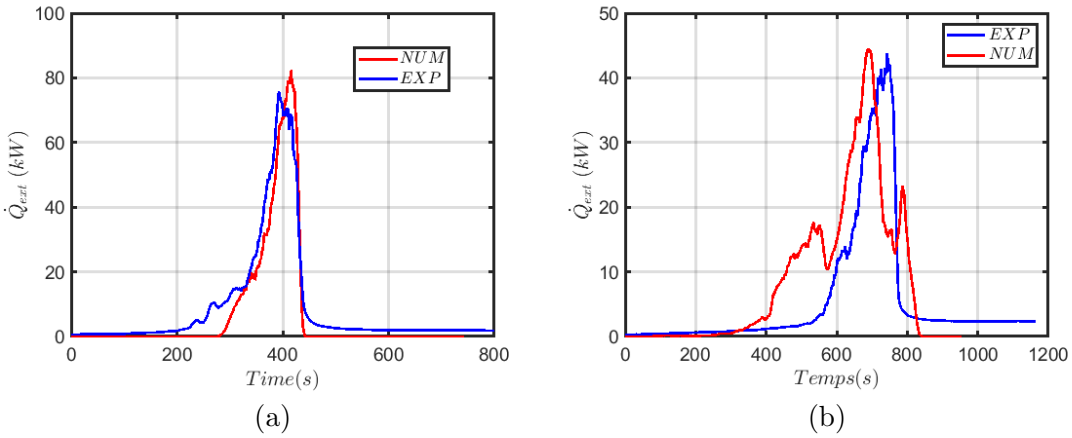

(a) (b)

Figure 8. Comparison between the numerical and experimental variation of the heat release rate outside the compartment in the case of a 15 cm pool with a ventilation factor of (a) 0.0481 $m^{5/2}$, (b) 0.017 $m^{5/2}$.

Figure 8 shows the comparisons between experimental and numerical data for two different cases, for $D = 15$ cm and two ventilation factors equal to 0.0481 $m^{5/2}$ and 0.017 $m^{5/2}$. The HRR outside the compartment is plotted as a function of time. The comparison shows an excellent agreement in Figure (8-a), which is not surprising for this moderately under-ventilated case, well described by FDS since the HRR inside the compartment was also well reproduced. The agreement is more questionable in (8-b), for which the under-ventilation is more severe.

In order to extend the comparison, the maximum outside HRR is plotted in Figure 9 as a function of the ventilation factor, comparing experimental results and numerical predictions. Here again, it can be seen that the comparison shows a reasonable agreement for all the pool diameters, because it concerns maximum values, better captured in all the regimes, than instantaneous or local values.

Results for temperature distributions and flow dynamics are now discussed in the next section to focus on local variables.

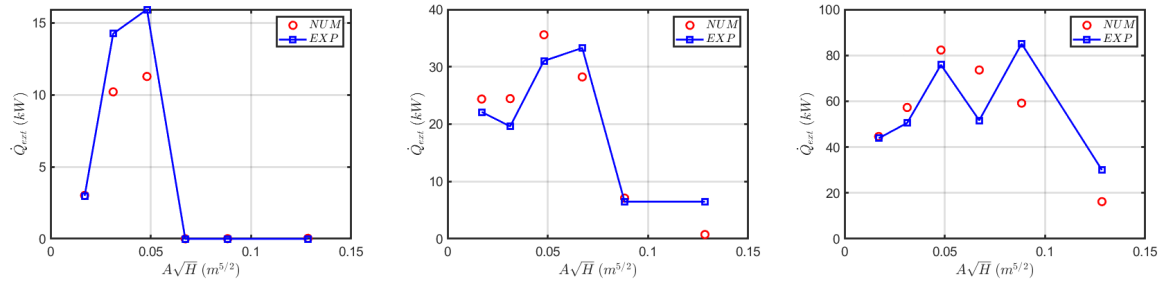

(a) D = 11 cm (b) D = 13 cm (c) D = 15 cm

Figure 9. Comparison between the numerical and experimental variation of the maximum heat release rate outside the compartment versus the ventilation factor for the different pool diameters, (a) D= 11 cm, (b) D= 13 cm, (c) D= 15 cm.

4.3. Temperature distributions and flow dynamics

Figures 10 and 11 present the variation of the dimensionless temperature $\theta = (T - T_0)/(T_{max} - T_0)$ profiles at different times, for pool fires with diameter $D = 15\,cm$ and door heights equal to $H = 60\,cm$ and $H = 10\,cm$ respectively. To ensure the clarity of the figures the temperature profiles were shifted by $\theta = 1$, $\theta = 2$, $\theta = 3$, $\theta = 4$, $\theta = 5$ representing t=100 s, 200 s, 300 s, 447 s and 470 s respectively.

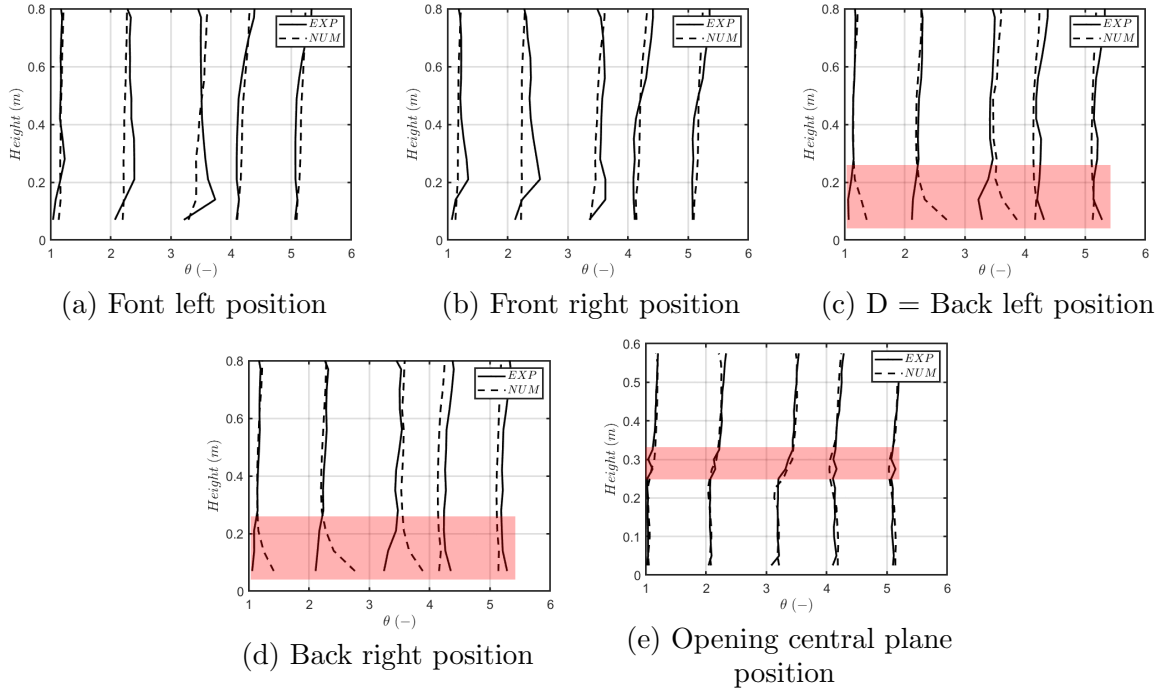

(a) Font left position (b) Front right position (c) D = Back left position

(d) Back right position (e) Opening central plane position

Figure 10. Comparison between the numerical and experimental temperature profiles for $D = 15\,cm$ and $H = 60\,cm$ at t=100 s, 200 s, 300 s, 447 s and 470 s.

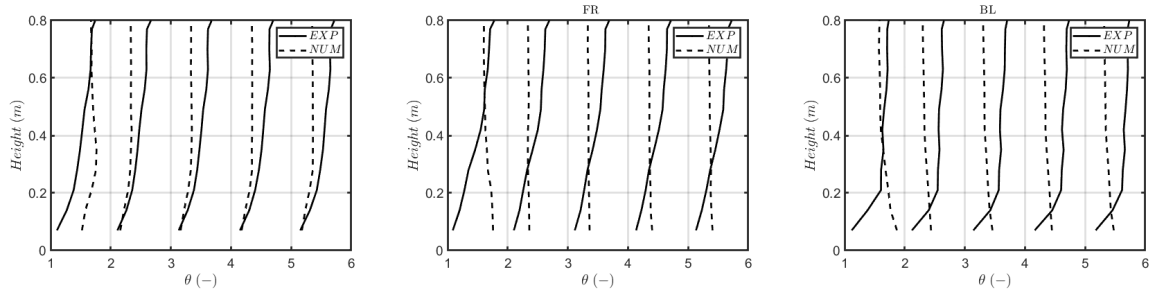

(a) Font left position (b) Front right position (c) D = Back left position

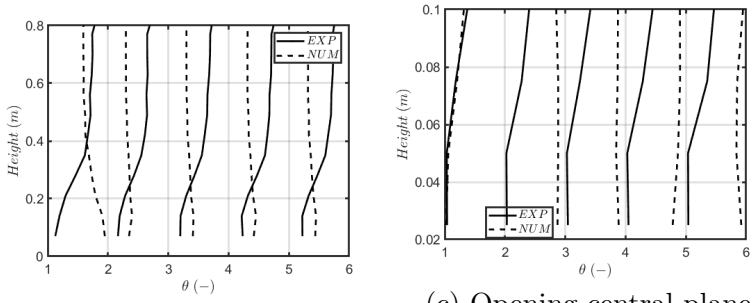

(c) Back right position (c) Opening central plane position

Figure 11. Comparison between the numerical and experimental temperature profiles for $D = 15\,cm$ and $H = 10\,cm$ at t=100 s, 200 s, 300 s,447 s and 470 s.

Analysing Figure 10 we can identify three different behaviours depending on the position. For the thermocouples trees located in the front left (10a) and right positions (10b), the experimental and numerical temperature profiles are in a good agreement. For the thermocouple trees located in the back left (10c) and right (10d) positions, two zones can be distinguished. In the lower part of the profiles (emphasized by the red area), the simulated temperatures are higher than the experimental ones. This behavior is induced by the motion of the flame. In fact, numerically we observe that the flame is leaning further back than what was observed experimentally. As a result, the flame impacts the thermocouples, causing high temperatures. For thermocouples located in the upper part, simulated and experimental temperatures are in good agreement. Finally, for thermocouple tree situated at the door (10e), the simulated temperatures are in good agreement with the experimental ones, except for the part represented by the red area, which corresponds to the interface between the hot and cold layers. This reflects the difficulty of characterizing this region of strong gradient. A particular attention must be also paid to the cases for which we have observed extinction. As shown in Figure 11, the temperature profiles inside the compartment are numerically underestimated, while the temperature profiles at the door are numerically overestimated. In fact, this is due to the distribution of the HRR between inside and outside the compartment, and to the fact that numerically,

5. Conclusions

In this study, the combustion regimes in compartment fires have been analysed numerically and experimentally. Thanks to temperature, gas concentration, heat flux measurements as well as image recording of the external flames, the combustion regime in the compartment has been fully characterised. In particular, two complementary methods have been used to evaluate experimentally the fire heat release rate inside and outside the compartment. With these methods, it has been shown that the maximum HRR inside the compartment never exceeds

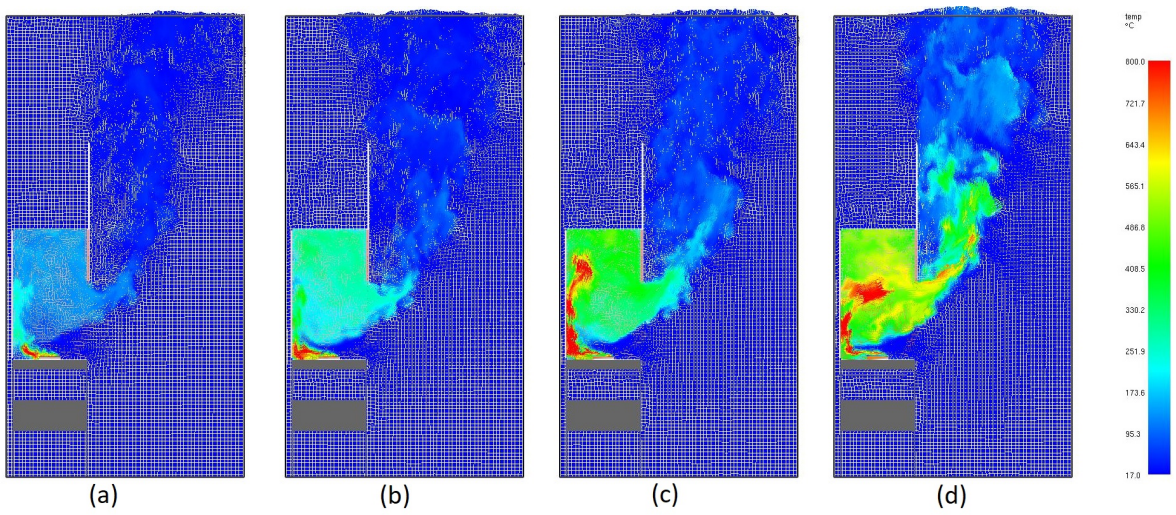

Figure 12. Illustration of the vector field and temperature contours for $D = 13\,cm$ and $H = 50\,cm$ at four moments: (a) 122s, (b) 386s, (c) 467s and (d) 528s.

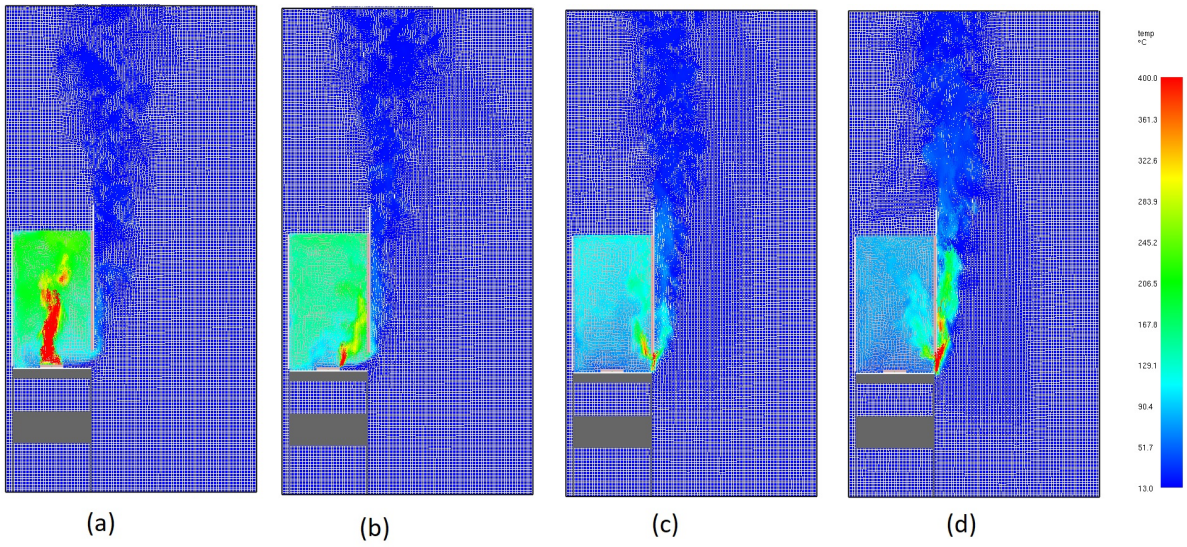

Figure 13. Illustration of the vector field and temperature contours for $D = 13\,cm$ and $H = 10\,cm$ at four moments: (a) 78s, (b) 117s, (c) 157s and (d) 392s.

900 $A\sqrt{H}$ which is significantly lower than the classical relation 1500 $A\sqrt{H}$. Moreover, the experimental data have been compared to numerical simulations carried out with the software Fire Dynamics Simulator. The comparisons between the experimental data and the numerical simulations were first based on maximum or integrated quantities such as maximum heat release rate inside the compartment. The agreement was surprisingly very good for all the points that have been tested which was an unexpected result, especially for under-ventilated conditions. Actually, the temporal variation of the HRR inside the compartment shows that the agreement was good when the compartment was well ventilated or moderately under-ventilated, while there was an obvious disagreement when the compartment was severely under-ventilated. In particular, the fire did not reach the maximum HRR at the same moment according to the experiment and the numerical simulation. The temperature distribution shows that there was

significant differences between the experiments and the simulations, even for the well ventilated cases. In the simulations, the flame was tilted and elongated by the air flow entering inside the compartment. This effect also exists experimentally, but seems to be much more pronounced in the numerical simulation. This observation demonstrates that the numerical code fails in reproducing the fire dynamics inside the compartment even for the well ventilated case. Moreover, in the case of severe under-ventilated conditions, a ghost flame takes place near the door and all the combustion occurs at that position. This behaviour is very different from what was observed experimentally. Further investigation should be conducted to improve the prediction. It seems that in the numerical simulation, the pressure inside the compartment is large and does not allow the fresh ambient air to go inside the compartment. All these observations call for a deeper exploration of the fluid dynamics of compartment fires in particular, how the pressure gradient at the door is handled by the numerical code. Sub-models used in FDS for ignition, combustion and extinction should be also further investigated.

Appendix A: Flame reconstruction method and $_{ext}$*evaluations*

Figure 14 shows an example of two images recorded during the experiment and the result of the reconstruction of this flame. The process used is as follows:

- Extraction of the two perpendicular images and transformation into a binary images.
- The flame surface is reconstructed by considering an elliptical cross-section.
- The view factor is calculated using a Monte-Carlo method.
- The radiative heat release rate is calculated using the following relation

$$\dot{Q}_{rad} = \frac{S \times \dot{q}''}{F} \ , \tag{9}$$

  where S is the surface area of the sensor, F is the view factor between the flame and the sensor, and $\dot{q}''$ is the measured radiant flux.
- the external flame heat release rate $\dot{Q}_{ext}$ is finally given by :

$$\dot{Q}_{ext} = \frac{\dot{Q}_{rad}}{\chi_{rad}} \ , \tag{10}$$

  with χ_{rad} is the radiative fraction estimated beforehand and given in table 2.

Table 2. Summary of radiative fractions for the various pan sizes.

D (cm)	5	8	9	11	13	15
χ_{rad}	0.36	0.31	0.28	0.31	0.32	0.39

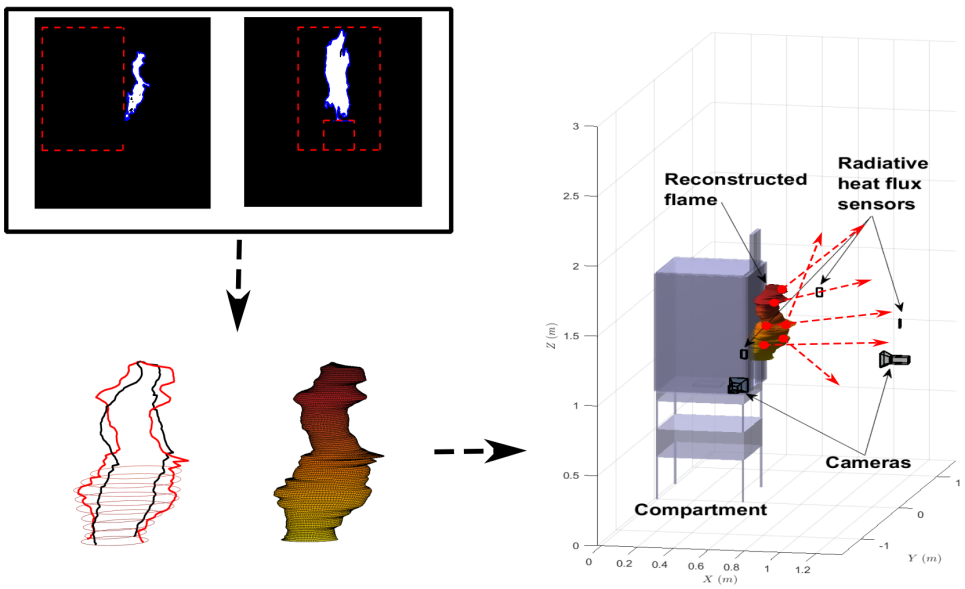

Figure 14. Flame reconstruction method.

References

[1] Dat Duthinh, Kevin McGrattan, and Abed Khaskia. Recent advances in fire–structure analysis. *Fire safety journal*, 43(2):161–167, 2008.

[2] Aatif Ali Khan, Asif Usmani, and José Luis Torero. Evolution of fire models for estimating structural fire-resistance. *Fire safety journal*, 124:103367, 2021.

[3] José L Torero, Agustin H Majdalani, Cecilia Abecassis-Empis, and Adam Cowlard. Revisiting the compartment fire. *Fire Safety Science*, 11:28–45, 2014.

[4] Junyi Li, Tarek Beji, Sylvain Brohez, and Bart Merci. Experimental and numerical study of pool fire dynamics in an air-tight compartment focusing on pressure variation. *Fire Safety Journal*, 120:103128, 2021.

[5] Junyi Li, Hugues Prétrel, Sylvain Suard, Tarek Beji, and Bart Merci. Experimental study on the effect of mechanical ventilation conditions and fire dynamics on the pressure evolution in an air-tight compartment. *Fire Safety Journal*, 125:103426, 2021.

[6] J Lassus, Léo Courty, JP Garo, E Studer, P Jourda, and P Aine. Ventilation effects in confined and mechanically ventilated fires. *International Journal of Thermal Sciences*, 75:87–94, 2014.

[7] Maxime Mense, Yannick Pizzo, Hugues Prétrel, Christine Lallemand, and Bernard Porterie. Experimental and numerical study on low-frequency oscillating behaviour of liquid pool fires in a small-scale mechanically-ventilated compartment. *Fire Safety Journal*, 108:102824, 2019.

[8] Tarek Beji, Juan Hidalgo Medina, Talal Fateh, Jason Floyd, Hugues Prétrel, and Anthony Hamins. Compartment fires: Challenges for fire modeling as a tool for a safe design (iafss workshop, april 2021). *Fire Safety Journal*, page 104109, 2024.

[9] Bjorn Karlsson and James Quintiere. *Enclosure fire dynamics*. CRC press, 2022.

[10] Bouaza Lafdal, Rabah Mehaddi, Pascal Boulet, Elmehdi Koutaiba, and Tarek Beji. Oscillatory burning regime in a gas-fueled compartment fire. *Fire Safety Journal*, 142:104045, 2024.

[11] Kunio Kawagoe. Fire behaviour in rooms. 27:1–70, 1958.

[12] PH Thomas and AJM Heselden. Behaviour of fully developed fire in an enclosure. *Combustion and Flame*, 6:133–135, 1962.

[13] Philip Humphrey Thomas, AJM Heselden, and Margaret Law. *Fully-developed compartment fires: Two kinds of behaviour*. HM Stationery Office, 1967.

[14] Clayton Huggett. Estimation of rate of heat release by means of oxygen consumption measurements. *Fire and materials*, 4(2):61–65, 1980.

[15] Arnaud Trouve and Yi Wang. Large eddy simulation of compartment fires. *International Journal of Computational Fluid Dynamics*, 24(10):449–466, 2010.

[16] S Vilfayeau, N Ren, Y Wang, and A Trouvé. Numerical simulation of under-ventilated liquid-fueled compartment fires with flame extinction and thermally-driven fuel evaporation. *Proceedings of the Combustion Institute*, 35(3):2563–2571, 2015.

[17] Bouaza Lafdal, Racha Djebbar, Pascal Boulet, Rabah Mehaddi, ElMehdi Koutaiba, Tarek Beji, and Jose Luis Torero. Numerical study of the combustion regimes in naturally-vented compartment fires. *Fire Safety Journal*, 131:103604, 2022.

[18] Kevin B McGrattan, Glenn P Forney, Jason Floyd, Simo Hostikka, and Kuldeep Prasad. *Fire dynamics simulator (version 4)–user's guide*. US Department of Commerce, Technology Administration, National Institute of . . . , 2005.

[19] Kevin B McGrattan, Howard R Baum, and Ronald G Rehm. Large eddy simulations of smoke movement. *Fire safety journal*, 30(2):161–178, 1998.

[20] Bart Merci and Karim Van Maele. Numerical simulations of full-scale enclosure fires in a small compartment with natural roof ventilation. *Fire safety journal*, 43(7):495–511, 2008.

[21] B. J. McCaffrey, J. G. Quintiere, and M. F. Harkleroad. Estimating room temperatures and the likelihood of flashover using fire test data correlations. *Fire Technology*, 17(2):98–119, May 1981.

[22] M Akasha Azhakesan, TJ Shields, GWH Silcock, JG Quintiere, and Northern Ireland. An interrogation of the mqh correlation to describe centre and near corner pool fires. *Fire Safety Science*, 7:371–382, 2003.

[23] Bouaza Lafdal. *Étude expérimentale et numérique des feux sous-ventilés*. PhD thesis, Université de Lorraine, 2022.

[24] K Steckler and D Corley. An assessment of fire induced flows in compartments. *Fire Science and Technology*, 4(1):1–14, 1984.

[25] Marc Janssens and Hao C Tran. Data reduction of room tests for zone model validation. *Journal of Fire Sciences*, 10(6):528–555, 1992.